Biochimica et Biophysica Acta, 981 (1989) 343–350
Elsevier

BBA 74422

Single potential-dependent K^+ channels and their oligomers in molluscan glial cells

V.I. Gelctyuk and V.N. Kazachenko

Institute of Biological Physics of the U.S.S.R. Academy of Sciences, Pushchino (U.S.S.R.)

(Received 6 February 1989)

Key words: Patch clamp; Potassium ion channel; Multiple conductance state; Channel degradation; (Molluscan glial cell)

Single K^+ channels were studied using the patch-clamp method. A potential-dependent K^+ channel of large conductance (about 100 pS at 100 mM of KCl on both membrane sides) was detected. Some properties of the channel (current–voltage relations, kinetic parameters, etc.) are presented. The channel was found to have about 16 resolvable quantized conductance substates. The data are confirmed by spontaneous channel degradation, i.e., spontaneous splitting of the channel conductance into independent conductance oligomers. Some properties of the conductance oligomers of different order are described. The degree of potential dependency of the conductance oligomer parameters is a function of the number of subunits constituting the oligomer, i.e., the larger the number of subunits the more the degree of potential dependency. The data obtained are in agreement with a hypothesis that the channels studied are clusters (aggregates) of elementary channel subunits.

Introduction

In earlier papers [1–4], K^+ and Cl^- channels in the molluscan neurones were shown to have 16 resolvable quantized conductance substates. As a rule, all the substates are interrelated, thus the channel transitions between the substates are highly cooperative. However, the cooperativity of the channel transitions disintegrates in some cases and channel uncoupling is observed. The phenomenon appears as a breakdown of the original channel into several small independent channels. Uncoupling seems to proceed in a step-like manner. First, the original channel conductance breaks down into two independent halves. Then each half breaks down into the next pair of independent conductance halves, and so forth. Finally, the channel operates as a sum of small independent channels. Other pathways of the channel uncoupling are possible [1–4].

Thus, the single ionic channels studied were termed as 'functional' clusters including about 16 resolvable subconductance states (or subunits) [2]. Each elementary channel subunit probably has its own gating mechanism, and the channel cluster has a particular gating mechanism for synchronization. A similar model was recently proposed for the K^+ channels in renal tubules [5].

In molluscan glial cells, a K^+ channel with striking potential dependency of the kinetic characteristics was found [6]. This channel is not activated by internal Ca^{2+}, since neither the absence nor the presence of Ca^{2+} at the inner membrane side has any appreciable effect on the channel activity. The channel is highly selective for K^+ as compared to other monovalent cations (for example, K^+ penetrates the channel about 10-times better than Na^+).

Similarly to K^+ and Cl^- channels in the molluscan neurones, the potential-dependent K^+ channel in the glial cells has about 16 resolvable subconductance states, the transitions between them being a cooperative process [6]. However, in some cases, uncoupling of the original channel into several independently operating fractions ('conductance oligomers') was observed. The properties of the conductance oligomers differ essentially from those of the original channel. In this paper some characteristics of the potential-dependent K^+ channel and its oligomers are compared and discussed.

Materials and Methods

Isolation of glial cells

The glial cells were isolated from fresh-water mollusc *Lymnaea stagnalis* brain after pronase pretreatment

Correspondence: V.N. Kazachenko, Institute of Biological Physics of the U.S.S.R. Academy of Sciences, Pushchino, Moscow Region, 142292, U.S.S.R.

(0.35%, 0.1–0.5 h, 20–22° C) using metallic needles and glass pipettes. The glial cells (10–30 μm in diameter) surround the molluscan neurones and are normally attached to them. The glial cells were distinguished from the smaller neurones by the following indications. (a) The glial cells are colourless, whereas the neurones from this molluscan species are yellow or orange. (b) The neurones possess an elongated second antennal segment, whereas the glial cells have only a great number of thin appendices. (c) The glial cells usually contain several dark pseudocytosomes (2–5 μm in diameter) which are visible under the light microscope.

Recording

The experiments were carried out using the patch-clamp method ('inside-out' mode) [7]. The pipettes were fabricated from borosilicate glass. The tip diameter of the fire-polished pipettes was less than 1 μm. The pipette resistance was 20–100 MΩ. Gigaseals were obtained by applying negative pressure (1–5 kN/m^2) to the pipette. The resistance of the gigaseal was equal to 20–100 GΩ. Currents are described using the physiological sign convention, i.e., the currents flowing from the internal membrane side (from the bath) to the external side (to the pipette) are taken as positive and displayed upwards. Liquid junction potentials were 1–3 mV and were neglected. The experiments were performed using a special bath (about 0.1 ml) providing continuous exchange of the bath solutions (several bath vols per s). Signals were low-pass filtered at 1–2 kHz (−3 dB, 4-pole Bessel) and registered by a photorecording system. The data were analysed by hand. The temperature was maintained at 20–22° C.

Solutions

The pipette was filled with normal physiological solution containing (in mM): NaCl 50/KCl 1.5/$CaCl_2$ 4/$MgCl_2$ 1.5; the pH was adjusted to 7.5 by Tris-HCl (2.5 mM). The inner side of the patch membrane was superfused by standard bath solution (in mM): KCl 50/Hepes-KOH 2.5 at pH 7.1–7.2.

Results

Kinetic parameters of the potential-dependent K^+ channel

Fig. 1A shows single-channel records at different levels of the membrane potential (V). The currents display burst-like behaviour. Fast current fluctuations are observed during the bursts. Sometimes, current substates are registered (Figs. 1A and 1B). Preliminary analysis showed that the potential-dependent K^+ channel has about 16 cooperatively related conductance substates [6].

To characterize the channel activity, the following average parameters were measured (Fig. 1): burst duration (t_b); duration of interburst interval (t_i); duration

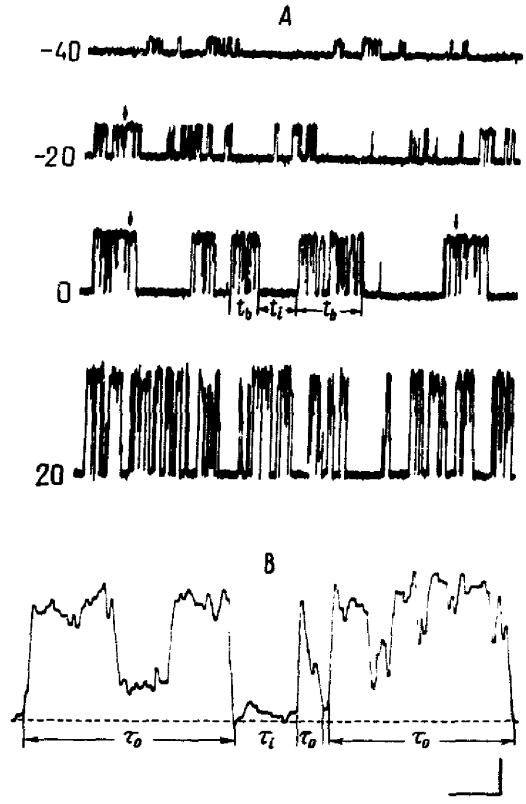

Fig. 1. Recordings of outward currents through single K^+ channels. A. The currents at different membrane potentials were recorded several seconds after shifting of the membrane potential from −50 mV to the potentials indicated (in mV) near the recordings. Horizontal arrows show some values of t_b (burst duration) and t_i (interburst interval). Vertical arrows indicate some current sublevels. The pipette was filled with normal physiological solution (see Materials and Methods); the bath contained 50 mM of KCl. Filtering, 200 Hz. B. The currents recorded at high sweep speed. Dashed line indicates zero current level. Horizontal lines determine some values of τ_o (open time) and τ_i (closed time). The pipette was filled with normal physiological solution; the bath solution contained 1 M of KCl. $V = 100$ mV. Filtering, 1.5 kHz. Calibrations: 1 pA and 150 ms (A); 12 pA and 3 ms (B). The data in (A) and (B) were obtained from different patches.

of single-current impulse (τ_o); and duration of gaps between single-current impulses within the bursts (τ_i). In addition, the probability of the channel open state (P_o) was determined as follows:

$$P_o = \sum \tau_o / T \qquad (1)$$

where T is a sampling duration.

Determination of the kinetic parameters is complicated due to the existence of the channel subconductance states. Fig. 1B shows the channel-current records obtained at high sweep speed and high K^+ concentration (1 M). The currents exhibit a great number of substates. τ_o was measured as the interval between the nearest closed states; the channel was believed to be closed when the current substate did not exceed 10% of the maximal current level. The method is justified by

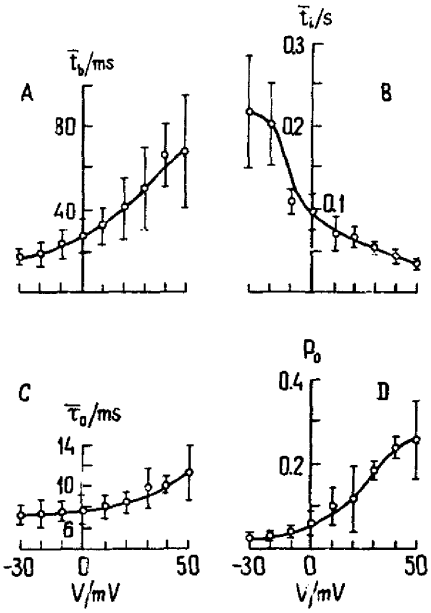

Fig. 2. Potential dependence of kinetic characteristics of the whole K^+ channel. $\bar{t}_b$ $\bar{t}_i$, $\bar{\tau}_o$ and P_o are, respectively, average values of the burst duration, interburst intervals, single open duration, and the probability of the channel open state (see text). Each point of the plots represents an average value from three to five patches. Error bars give ± S.D. The bath solution contained 50 mM of KCl.

the stepwise form of increasing and falling phases of the current impulses which reflect probably the current transitions between the substates. Sometimes, due to the limited bandwidth (1–2 Hz), it was difficult to decide which channel state (fully or partially closed/open) the registered current level corresponded to. For this reason, some measured values of τ_o probably represent short-lived impulse bursts separated by closed times no longer than 0.3–0.5 ms.

To obtain the values of the intervals between neighbouring pulses and those of interburst gaps all shut periods in the channel activity were taken into account. The distribution of this parameter can be approximated by two exponents with the time constants of approx. 5 ms and several tens of milliseconds [6]. The shorter time constant is believed to characterize the intervals between single openings, τ_i, and the longer one represents the intervals between the bursts, t_i. In accordance with the average value of $\bar{\tau}_i$ (about 5 ms), the bursts were defined as single impulse groups separated by closed intervals being at least 50 ms. Averaged values of t_b, t_i, τ_o and τ_i were obtained from 100–200 measurements and used for the analysis.

Fig. 2 demonstrates the potential dependences of the kinetic parameters. The parameters $\bar{t}_b$, $\bar{\tau}_o$ and P_o increase, and $\bar{t}_i$ decreases with the membrane potential. In the range from −30 to 50 mV $\bar{t}_b$, $\bar{t}_i$ and P_o change 3–8-times, whereas $\bar{\tau}_o$ increases only 1.5-fold. $\bar{\tau}_i$ does not depend on the membrane potential and has a constant value of 5.2 ± 1 ms (S.D., $n = 4$).

Degradation of the channel conductance

We found that the single-channel conductance degrades spontaneously in a way supporting the multiplicity of the conductance substates.

Degradation is seen as a splitting of the original set of interrelated channel substates into several independent groups of the conductance substates (conductance oligomers). Each independent group of substates, in turn, consists of several interrelated multiple sublevels. The total sum of the substates in all conductance oligomers formed during the channel degradation is equal to the number of substates of an original channel (i.e., about 16). In some cases the degradation is complete, that is, the original channel conductance breaks into independent elementary steps, monomers. The channel degradation is irreversible under given experimental conditions.

Fig. 3 provides an example of the channel degradation. Immediately after excision of the patch, the channel forms usual current impulses corresponding to the whole-channel conductance of about 40 pS (Fig. 3A). The current sublevels are short-lived and interrelated.

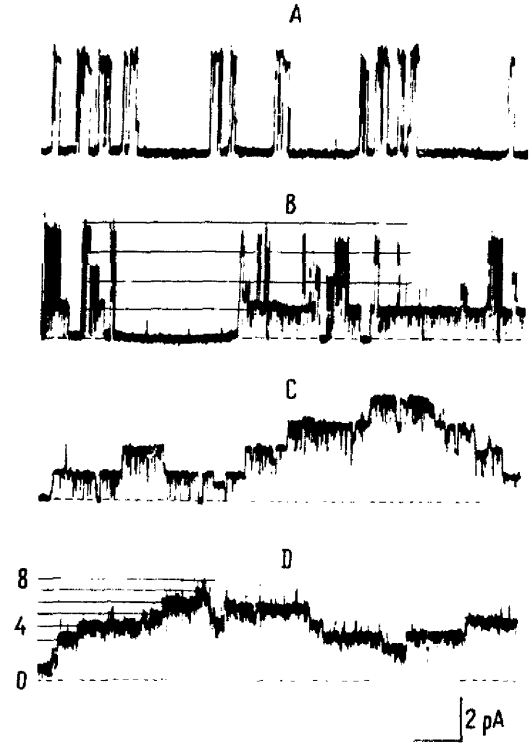

Fig. 3. Degradation of the channel conductance. A. Initial current impulses registered at the beginning of the experiment. B. 25 min later, the conductance broke up into four slightly interrelated substates. C. Breakdown of the channel conductance into four independent tetramers (1 h after the beginning of the experiment). D. The channel activity at the end of the experiment (1.5 h after it began). Horizontal lines show the current sublevels. The bath contained 50 mM of KCl. $V = 50$ mV. Time calibrations: 150 ms (A), 300 ms (B,C) and 75 ms (D). Low-pass filtering, 200 Hz. Dotted lines indicate the zero-current level.

25 min later, the channel activity suddenly changes and the channel begins to display four main prolonged substates (Fig. 3B). The conductance of the prolonged states correspond to about 0.25, 0.5, 0.75 and 1.0 of the upper level of the original channel conductance. Nevertheless, the transitions between the prolonged substates are still interrelated to some extent and the probability of instantaneous current jumps of a whole amplitude is still high. With time, the interrelation between the prolonged substates disappears. Fig. 3C shows the channel activity 1 h after the experiment was started. Here, the channel activity looks like the activity of four independent channels with the conductances of about 0.25 of the original channel conductance. In addition, each independent oligomer (tetramer) has its own interrelated substates. Finally, the original channel conductance breaks down into eight independent dimers (Fig. 3D). In this experiment, subsequent degradation stages were not observed, but, in general, splitting of the channel conductance into up to 16 independent subunits is possible.

Sometimes the channel degradation is accompanied by the disappearance of activity in some oligomers. The probability of this process increases after splitting of the channel conductance into small oligomers. In view of the fact that the different stages of the channel degradation are not synchronized, various combinations of conductance oligomers could be observed.

Independent conductance oligomers arising during the channel degradation seem most likely to be the derivatives of one and the same original conductance due to the following reasons. (a) The appearance of the oligomers of reduced orders is accompained by the disappearance of the original channel conductance. (b) The total conductance of the oligomers arising in the course of the degradation does not exceed the conductance of an original channel. (c) The values of the elementary conductance step of the oligomers are similar to that of the original channel.

Some other phenomena were also observed during the channel degradation. (a) Sometimes the degradation begins as a prolongation of the lifetime of some selected conductance sublevels and attenuation of cooperativity between them. With time, the interrelation between the prolonged substates may be lost completely and independent conductance oligomers may arise. (b) In other cases, several minutes after excision of a patch, the whole channel conductance suddenly breaks down into a great number of independent small conductance oligomers. (c) The degradation may begin from several minutes to several hours after excision of a patch.

'Pre-existent' conductance oligomers

It is possible that the degradation is an intrinsic property of the channels and exist in the membrane prior to formation of the patch-pipette contact. This

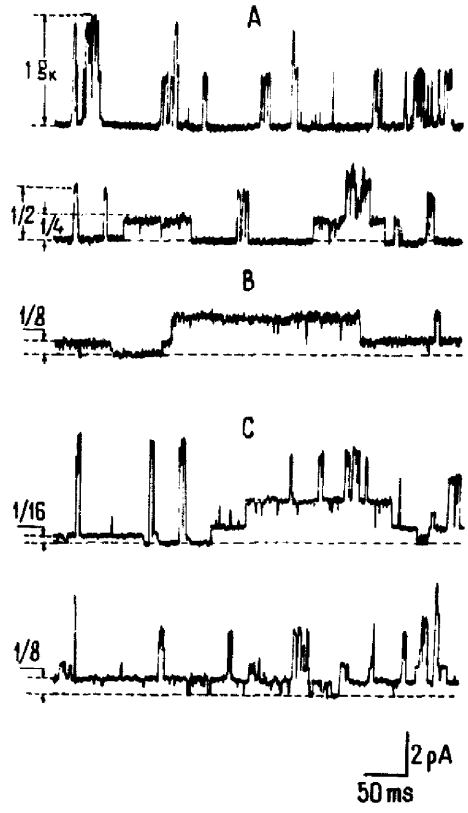

Fig. 4. Current recordings from 'pre-existent' K^+ channels of different conductance. A. Three independent channels with the conductances (in pS): 37, 19 and 8.5. B. Two active channels of 10 and 5 pS in the conductance. C. Five independent channels with the multiple conductances (in pS): 2.5, 6, 9, 19 and 37. The recordings in A, B and C were obtained from three different patches. Values near the recordings indicate some conductance levels as fractions of the maximal (whole) channel conductance. Bath contained 50 mM of KCl. $V = 50$ mV. Filtering, 200 Hz.

assumption is based on the observation of the single ionic channels of different conductance ('pre-existent' oligomers) shortly after formation of gigaseal contact. The 'pre-existent' oligomers have different sets of multiple conductance substates, and the elementary conductances are the same as that of the whole potential-dependent channel.

Fig. 4 shows the current recordings from three active patches providing an example of five main kinds of the 'pre-existent' oligomer. The upper two traces (the first patch represent the activities of three independent K^+ channels. The channel conductances are in the following approximate ratios: 1 : 0.5 : 0.25. The channel of the largest conductance (about 40 pS at 50 mV) is similar to the whole K^+ channel described above. The other two channels may be regarded in the context of this paper as an octamer and tetramer. The middle trace, B, is the current recorded from a second patch with two active K^+ channels. The channel conductances comprise approx. 0.25 and 0.13 of the whole channel conductance and may be defined as a tetramer and dimer, respec-

tively. Finally, the bottom two traces (Fig. 4C) show activity of a third patch with five main types of the K^+ channel. The conductance ratios form approximately the following sequence:

1:1/2:1/4:1/8:1/16 (2)

The smallest channel may be defined as a monomer.

In accordance with the sequence (2), the average values of the main conductance oligomers at 50 mV are as follows (in pS): 39 ± 2.5 ($n = 5$), 21.6 ± 1.6 ($n = 4$), 12 ± 1.2 ($n = 5$), 6.3 ± 1.0 ($n = 4$), 3.1 ± 0.9 ($n = 3$). The probabilities of occurrence of the channels as the whole channel, octamer, tetramer, dimer and monomer are, respectively, 0.1, 0.15, 0.5, 0.1 and 0.05. As can be seen, the tetramers are the most plausible conductance oligomers.

In most cases, the properties of the 'pre-existent' oligomers are identical to those of homological conductance oligomers described above. Thus, the 'pre-existent' oligomers are likely to be fragments of the whole-channel conductance arising from to the channel degradation. However, it remains uncertain whether the degradation takes place before the experiment or arises due to gigaseal contact.

Some properties of the oligomers

The following observations were made on the patches containing only a single oligomer of any order.

Fig. 5 shows the $I-V$ curves for the whole channel and those for the monomer, tetramer and octamer. The comparison of the data allowed us to make the following conclusions: (a) The current-reversal potentials obtained from the extrapolated $I-V$ curves are near the K^+ equilibrium potential, i.e., different conductance

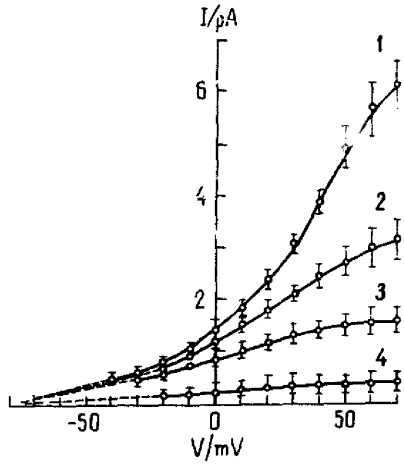

Fig. 5. Current–voltage relationships of the whole channel (1), octamer (2), tetramer (3) and monomer (4). The pipette solution was filled with a normal physiological solution; the bath contained 50 mM of KCl. Each curve represents the averaged data from three to five patches.

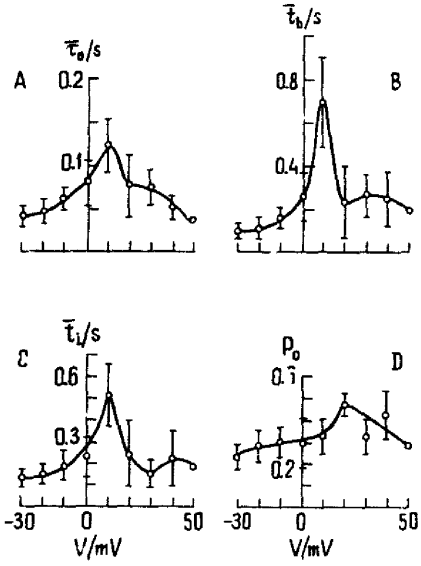

Fig. 6. Potential dependences of kinetic parameters of the tetramer. The quantities $\bar{t}_b$, $\bar{t}_i$, $\bar{\tau}_o$ and P_o are the same as those defined in the legend to Fig. 2. Each point represents an averaged value from four patches. Error bars give ± S.D. The measurements were made on the patches containing only the single active tetramer without activity of other channels. The pipette was filled with the normal physiological solution; the bath solution contained 50 mM of KCl.

oligomers are highly selective for K^+. (b) For all types of oligomer the currents tend to saturate as the membrane potential increases. However, the curve inflections associated with the current saturation occur at different potential values. The $I-V$ curve for the whole channel bends at about 80–100 mV, whereas those for the octamer, tetramer and monomer bend at 50, 20–30, and 9–10 mV, respectively. (c) The potential dependency of the currents is larger for oligomers of higher order. Exact proportionality between oligomer order and current values is observed at potentials about or greater than 50–70 mV.

Kinetic parameters of the tetramers were analysed. Their values were measured in the same way as those of the whole channel. However, unlike the whole channel, the tetramer openings in the bursts were separated by comparatively short closures ($\bar{\tau}_i \approx 1$ ms) and the interburst intervals were longer (see Fig. 4); thus, determination of the kinetic parameters was comparatively simple.

Fig. 6 illustrates the potential dependences of the kinetic characteristics of the tetramers. All relationships are bell-shaped with maxima at near 10 mV, whereas the corresponding relationships of the whole channel showed a monotonous voltage dependency (Fig. 2). For the tetramers, the quantities $\bar{t}_b$ and $\bar{\tau}_o$ were about 10-fold larger than those for the whole channel and $\bar{t}_i$ was about 1.5-times larger. Excluding the narrow voltage range from 0 to 20 mV, the kinetic parameters of the tetramer were almost independent of voltage.

Oligomers of lower order had similar properties. The values of the kinetic parameters of octamers ranged between those of the whole channel and of the tetramer. Thus, reduction of the oligomer order is accompanied by a progressive increase in the kinetic parameters and a decrease in the degree of voltage dependence of the channels' conductance and kinetic characteristics.

Recently, French and Stockbridge [8] have described five Ca^{2+}-independent K^+ channels with conductances from 21 to 235 pS in symmetric 140 mM potassium solution in human and avian fibroblasts. The channels had different potassium:sodium permeabilities. The largest channel (235 pS) had a steep bimodal voltage dependence of P_o, whereas the remaining four channels were voltage-insensitive. The authors did not discuss the possible origin of the channels.

Discussion

We have described some properties of a potential-dependent K^+ channel and its conductance oligomers in molluscan glial cells. The presence of potential-dependent channels in glial cells seems to be unexpected, since until recently the glial cells have been considered to be electrically nonexcitable partners of the neurones possessing presumably a potential-independent K^+ conductance [9]. However, as MacVicar [10] has noted, the pronounced K^+ conductance could shunt and mask other potential-dependent responses in glial cells. Indeed, recently, a Ca^{2+} conductance and prolonged action potentials were found in cultured glial cells using blockers of K^+ channels [10]. Potential-dependent Na^+ and K^+ channels have been detected in mammalian Schwann cells [11]. At the same time, potential-independent K^+ channels have been registered in oligodendrocytes [12].

Thus, the properties of ion channels in glial cells are more complex than has been imagined until recently.

Subconductance states

The main result of this paper is the detection of multiple conductance substates of the potential-dependent K^+ channel in molluscan glial cells. 16 quantized and cooperatively related substates are resolvable for the whole K^+ channel. The interrelated substates may degrade spontaneously into independent groups of the substates (conductance oligomers). On the other hand, 'pre-existent' oligomers of a different order and with properties similar to those of homological oligomers created due to the channel degradation have been registered.

Similar data have been obtained in our earlier studies. For example, the slow potential-dependent K^+ channel in the molluscan neurones also broke down into multiple conductance oligomers spontaneously and due to the application of internal Cd^{2+} [2]; elimination of external Ca^{2+} provoked uncoupling of the Cl^- channels in the molluscan neurones [4]. Under the given experimental conditions, the channel uncoupling was irreversible. However, in some cases, barium and thiol reagents restored the cooperativity of the channel transitions between the substates [13]. Great numbers of subconductance states were found in other types of ionic channel (see the review by Fox [14], and Ref. 15).

The properties of the multiple conductance substates demand an adequate channel model. The conductance of the whole potential-dependent K^+ channel is about 100 pS ($[K^+]_i = [K^+]_0 = 100$ mM). In accordance to the taxonomy offered by Latorre and Miller [16], this channel may be characterized as a maxi-channel. A surprising feature of the maxi-channels is their high ion selectivity at comparatively large channel conductance. To correlate these data, Latorre and Miller [16] have offered for the maxi-channels a special structure of the ionic pore with a wide capture area exposed to the aqueous diffusion region and the lumen of short tunnel. According to this model, independent and/or cooperative channel-current transitions between the substrates could be ascribed to fluctuations of linear sizes of the channel diffusion region and short tunnel.

Another possible mechanism of single-channel current regulation could be suggested by the data of Sakmann and co-workers [19] obtained for the AChR channels in adult and fetal forms of muscles. The authors have shown that unit channel conductance is influenced by a number of charged amino acids near the ends of the channel lining and membrane-spanning helices. In this case, fluctuations of an effective electrical charge of the channel macromolecular could result in corresponding fluctuations of the single-channel current between the substates.

In both channel models with a single ion pore the multiplicity of the current substates is not an essential property. It remains unclear why the substates are multiple and what is the mechanism of the channel degradation. Moreover, in the case of fluctuating charges, there is a possibility to diminish their influence on the channel current and the substates using the bath solutions of high ionic strength (ionic concentrations). However, our preliminary experiments with 1 M of KCl did not reveal any effect on the number and multiplicity of the current substates.

From our viewpoint, the properties of the channel substates may be described more adequately on the basis of the channel-cluster model [1–4] (see also Refs. 15, 17 and 18). In this model a so-called single channel of large conductance is regarded as being an aggregate (cluster) consisting of identical channel subunits (elementary channels or protochannels). The number of the channel subunits in the cluster equals the number of channel-conductive substates. Thus, the whole K^+ channel in the glial cells is believed to consist of 16 identical

channel subunits. Each elementary channel has its own ionic pore and gating mechanism. Normally, all channel subunits are interrelated and gate synchronously (cooperatively). The synchronous operation of the channel subunits gives the impression of activity of a large single channel.

The elementary conductance (conductance of a channel subunit) for the K^+ channels in the molluscan glial cells is about 6 pS ($[K^+]_o = [K^+]_i = 100$ mM, 20 °C). This value is close to the minimal conductance step of 4–8 pS (normalized to the same internal and external ion concentrations of 100 mM and 20 °C) obtained for a wide variety of ionic channels. Some of the examples are as follows: Na^+ channels in squid axon [20], tunicate egg [21] and rat brain neurones [22,23]; K^+ channels of delayed rectifier in myelinated nerve [24,25]; K^+ channels of anomalous rectifier in cultured rat myotubes [26], tunicate egg [21] and ventricular cells from guinea-pig heart [27]; K^+-Na^+ channels of ACh receptor in embryonic muscle cells [28], and cultured rat myotubes [29]; K^+-Na^+ channels of ACh receptor from *Torpedo californica* [30]; Cl^- channels in mouse spinal neurones activated by glycine and GABA [31]; Cl^- channels from *Torpedo* electroplax [32].

Oligomerization and the channel functions

Independently of the actual mechanism responsible for the subconductance states, we believe the channels studied to be 'functional oligomers'. The data show that a decrease of the conductance oligomer order leads to (1) an increase in the kinetic parameter values ($\bar{t}_b$, $\bar{t}_i$, $\bar{\tau}_o$, P_o) of the oligomers, and (2) diminution of the voltage sensitivity of these parameters with K^+ permeability remaining relatively high.

Changes in the degree of the voltage sensitivity of the oligomer parameters due to variation of the oligomer order (Fig. 6) is of special interest because voltage sensitivity is one of the main properties of the ionic channels in the electroexcitable membranes. The kinetic characteristics of the monomer, dimer and tetramer are practically voltage-independent, whereas the voltage sensitivity of the oligomers of higher order increases with the number of the oligomer subunits. The whole channel has the most pronounced voltage sensitivity. Thus, the oligomerization of the channel subunits is believed to have an important role in the acquisition of their voltage sensitivity (see also Ref. [15]).

Changes in the number of the subunits in a channel-cluster is accompanied by a modification of some other channel properties. For example, in the molluscan neurones, affinity of the slow whole potential-dependent K^+ channel to TEA as a blocker is several times lower than that of the octamer (halved channel) [33]. Similarly, in the molluscan neurones, inhibition of the lowest oligomers of the fast K^+ channel by Mg^{2+} is about 100-times higher than that of the whole channel [34].

Acknowledgement

We thank Mrs. O. Shvirst for her assistance with the English text.

References

1 Geletyuk, V.I. and Kazachenko, V.N. (1983) Dokl. Acad. Nauk. USSR 268, 1245–1247 (in Russian).
2 Kazachenko, V.N. and Geletyuk, V.I. (1984) Biochim. Biophys. Acta 773, 132–142.
3 Kazachenko, V.N. and Geletyuk, V.I. (1984) Biol. Membr. 1, 1253–1265 (in Russian).
4 Geletyuk, V.I. and Kazachenko, V.N. (1985) J. Membr. Biol. 86, 9–16.
5 Hunter, M. and Giebisch, G. (1987) Nature 327, 522–524.
6 Geletyuk, V.I. and Kazachenko, V.N. (1984) Biol. Membr. 1, 1204–1219.
7 Hamill, O.P., Marty, A., Neher, E., Sakmann, B. and Sigworth, F.J. (1981) Pflügers Arch. 391, 85–100.
8 French, A.S. and Stockbridge, L.L. (1988) Proc. R. Soc. Lond. B 232, 395–412.
9 Kuffler, C.W. and Nichols, J.G. (1977) in From Neurone to Brain (Magazanik, L.G., ed.), Mir, Moscow (in Russian).
10 MacVicar, B.A. (1984) Science 226, 1345–1347.
11 Shrager, P., Chin, S.Y. and Ritchie, J.M. (1985) Proc. Natl. Acad. Sci. USA 82, 948–952.
12 Kettenmann, H., Orkand, R.K., Lux, H.D. and Schachner, M. (1982) Neurosci. Lett. 32, 41–46.
13 Kazachenko, V.N. and Geletyuk, V.I. (1987) Biofizika 32, 73–78 (in Russian).
14 Fox, J.A. (1987) J. Membr. Biol. 97, 1–8.
15 Hymel, L., Striessing, J., Glossmann, H. and Schindler, H. (1988) Proc. Natl. Acad. Sci. USA 85, 4290–4294.
16 Latorre, R. and Miller, C. (1983) J. Membr. Biol. 71, 11–30.
17 Krouse, M., Schneider, G.T. and Gage, P.W. (1986) Nature 319, 58–60.
18 Schindler, H. and Schreibmayer, W. (1985) in Molecular Basis of Nerve Activity (Changeux, J.-P. et al., eds.), pp. 388–397, Walter de Gruyter, Berlin.
19 Mishina, M., Takai, T., Imoto, K., Noda, M., Takahashi, T., Numa, S., Methfessel, C. and Sakmann, B. (1986) Nature 321, 406–411.
20 Conti, F., DeFelice, L.F. and Wanke, E. (1975) J. Physiol. (Lond.) 248, 45–82.
21 Ohmori, H. (1981) J. Physiol. (Lond.) 311, 289–305.
22 Boheim, G., Hanke, W., Barhanin, J., Pauron, D. and Lasdunski, M. (1985) in Molecular Basis of Nerve Activity (Changeux, J.-P., et al., eds.), pp. 131–144, Walter de Gruyter, Berlin.
23 Harsthorne, R.P., Keller, B.U., Talvenheimo, J.A., Catteral, W.A. and Montal, M. (1985) Proc. Natl. Acad. Sci. USA 82, 240–244.
24 Hille, B. (1973) J. Gen. Physiol. 61, 669–686.
25 Begenisich, T. and Stevens, C.F. (1975) Biophys. J. 15, 843–846.
26 Ohmori, H., Yoshida, S. and Hagiwara, S. (1981) Proc. Natl. Acad. Sci. USA 78, 4960–4964.
27 Sakmann, B. and Trube, G. (1984) J. Physiol. (Lond.) 347, 641–657.
28 Hamill, O.P. and Sakmann, B. (1981) Nature 294, 462–464.
29 Takeda, K. and Trautmann, A. (1984) J. Physiol. (Lond.) 349, 353–374.

30 Schindler, H., Spillecke, F. and Neumann, E. (1984) Proc. Natl. Acad. Sci. USA 81, 6222–6226.
31 Bormann, J., Hamill, O.P. and Sakmann, B. (1987) J. Physiol. (Lond.) 385, 243–286.
32 Miller, C. and White, M.M. (1984) Proc. Natl. Acad. Sci. USA 79, 7749–7753.
33 Geletyuk, V.I. and Kazachenko, V.N. (1987) Biofizika 32, 859–873 (in Russian).
34 Kazachenko, V.N., Geletyuk, V.I. and Fomina, E.V. (1988) Dokl. Acad. Nauk. USSR 301, 997–1002 (in Russian).